Molecular Crystals and Liquid Crystals
Publication details, including instructions for authors and subscription information:
http://www.informaworld.com/smpp/title~content=t713644168

Dipole Dynamics of a Nano Doped Weakly Polar Liquid Crystal

R. Manohar[a]; Satya Prakash Yadav[a]; Abhishek Kumar Misra[a]; Kamal Kumar Pandey[a]
[a] Liquid Crystal Research Lab, Physics Department, University of Lucknow, Lucknow, India

First published on: 18 January 2011

To cite this Article Manohar, R. , Yadav, Satya Prakash , Misra, Abhishek Kumar and Pandey, Kamal Kumar(2011) 'Dipole Dynamics of a Nano Doped Weakly Polar Liquid Crystal', Molecular Crystals and Liquid Crystals, 534: 1, 57 — 68
To link to this Article: DOI: 10.1080/15421406.2011.536481
URL: http://dx.doi.org/10.1080/15421406.2011.536481

Mol. Cryst. Liq. Cryst., Vol. 534: pp. 57–68, 2011

ISSN: 1542-1406 print/1563-5287 online
DOI: 10.1080/15421406.2011.536481

Taylor & Francis
Taylor & Francis Group

Dipole Dynamics of a Nano Doped Weakly Polar Liquid Crystal

R. MANOHAR, SATYA PRAKASH YADAV, ABHISHEK KUMAR MISRA, AND KAMAL KUMAR PANDEY

Liquid Crystal Research Lab, Physics Department, University of Lucknow, Lucknow, India

The dielectric measurements of a weakly polarized nematic liquid crystal (D6AOB) were carried out in the frequency range 100 Hz to 40 MHz and in the voltage range from 0 to 40 V at 100 Hz. The dielectric data were measured for two principal alignments, homeotropic and planar. The angle β between the long molecular axis and dipole moment of the molecules is calculated from Cole-Cole plots using Onsager theory, both for pure and doped liquid crystal. Here is an attempt to discuss the $\Delta\varepsilon$ v/s voltage on the basis of piezoelectric strain, which is in good agreement with experimental results.

Keywords Dielectric anisotropy; dipole dynamics; nanoparticles; nematic liquid crystal

Introduction

In soft condensed matters, such as liquid crystals (LCs) and polymers, the fluctuation of their structure is large and their response to the external field gives detailed information about the molecular dipole dynamics of these materials. A wide variety of experimental methods are used to study the molecular dynamics of the LCs. In recent years, full-color and flat-screen liquid-crystal displays (LCDs), which are almost indispensable in many fields, have aroused much interest in the study of LCs. These LC devices are known to operate in the frequency region of few Hertz (Hz) to several mega-Hertz (MHz), which involves different modes of their molecular motions. Because these molecular motions involve both collective and noncollective types, dipolar studies prove to be a powerful tool to elucidate the Lcs molecular properties of liquid crystals [1,2].

Recently, modifications of the physical properties of LCs by doping nanoparticles have received much attention from the view point of the enhancement of the performance of elctro-optical LC devices. Reflecting these trends, several groups reported all heterogeneous LC suspensions using ferromagnetic particles; ferroelectric nanoparticles; fullerene; nanoparticles of metals such as Pd, Ag, Ag/Pd; inorganic nanoparticles

Address correspondence to Dr. Rajiv Manohar, Liquid Crystal Research Lab, Physics Department, University of Lucknow, University road, Lucknow 22607, India. E-mail: rajiv.manohar@gmail.com

of MgO; carbon nanotubes; and polymeric nanostructures [3,4]. Such doping structure motivates determinig the effect of zinc oxide nanoparticles (ZONPs) on the dipole dynamics and the molecular properties of LCs in view of excellent atomic and electrical properties of ZONPs [5]. The dispersion and alignment of ZONPs in LCs may improve the mechanical, electrical, thermal, and optical properties of bulk LC materials [6].

Dielectric anisotropy of LCs causes director reorientation in the applied electric field, which leads to the phenomenon of director reorientation in the electric field. This Fredericks effect is a well-known phenomenon that has numerous applications, most notably in LC displays [7–9]. On the other hand, in view of interdisciplinary relevance between LC physicists and chemists, it is useful to study the dynamics of LC molecular dipoles in the nematic range and near the phase transition range. The dipolar dynamics study of LCs with respect to various parameters such as temperature, frequency, voltage, etc., provides valuable information about the molecular arrangement, intermolecular interactions, and dynamics of reorientational motions. Hence deep insights of the dipole dynamics and dielectric anisotropy is required to understand the mechanism behind the variation of these properties with various parameters such as temperature, frequency, voltage, etc. [10,11].

The study of nematic LCs having weak dipole moments when doped with ZONPs may provide some additional information about the molecular properties [12,13]. In this investigation, inorganic ZONPs were dissolved in a weakly polar nematic LC at a low weight concentration to form a nano nematic suspension. Our aim is to study the influence of ZONPs on the dipolar motions of nematic LC molecules and on anisotropy of the system.

Experimental Details

Materials

A ZONPs-doped LC suspension of a nematic LC host, 4,4′-di hexyl azoxy benzene (D6AOB) were used for the present investigations. The chemical structure of the nematic host sample is shown in Fig. 1 with the following phase transition sequence

$$\text{Nematic } (22^{\circ}\text{C}) \rightarrow \text{Isotropic } (51^{\circ}\text{C}).$$

The host sample was purchased from Flintron Laboratories. The nanoparticles (provided by the Nano Phosphor Centre, Physics Department, University of

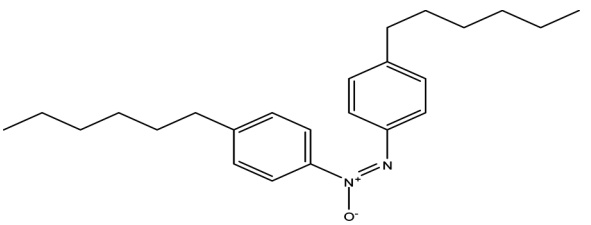

Figure 1. Chemical structure of D6AOB (4,4′-di hexyl azoxy benzene) molecule.

Allahabad, Allahabad, U.P., India) were synthesized by a chemical technique based on hydrothermal method. The crystallite sizes, estimated by X-ray diffraction (XRD) were found to be nearly 14 nm, whereas (tunnelling electron microscopy/scanning electron microscopy) (TEM/SEM) studies showed formation of uniform nanorods [14]. At room temperature, nanoparticles of ZnO are wide bandgap (3.38 ev) semiconductors in nature and also have piezoelectricity [5].

Preparation of the Sample Cell

We have used planar as well as homeotropic modes of LCs for our dielectric studies. The sandwiched-type (capacitor) cells were made using two optical plane glass substrates coated with conducting indium tin oxide (ITO) layers. To obtain planar alignment, the conducting layer was treated with the adhesion promoter and coated with polymer nylon (6/6). After drying the polymer layer, two substrates were rubbed unidirectionally by a velvet cloth. The substrates were then placed one over another to form a capacitor. The cell thickness was fixed by placing a Mylar spacer (5 μm in our case) in between and sealing with an ultraviolet (UV) sealant. Similarly for homeotropic alignment, the substrate was cleaned with acetone and then simply coated with the dilute solution of lecithin. The substrates were dried at 200°C for 10 h before assembling the cell. The detailed method for preparation of sample cells with planar and homeotropic alignment is discussed in our earlier papers [15–17]. The empty sample cells were calibrated using analytical reagent (AR)-grade CCl_4 and benzene as standard references for dielectric studies. The LC suspension was prepared by a nonsynthetic chemical method in the weight ratio 1:100 (i.e., 1% concentration of nanoparticles in nematic liquid crystal). The assembled cells were filled with the suspension and pure LC at a temperature 10°C higher than the isotropic temperature of the liquid crystal using a capillary method.

Dielectric Measurement

Dielectric measurements were carried out using a computer-controlled gain/phase analyzer (HP 4194A, Instech, USA) with a temperature controller attached in the frequency range 100 Hz to 10 MHz. The dielectric measurements were carried out as a function of temperature by placing the sample on a computer-controlled hot plate (HCS-302, Instec Co.). The temperature stability was better than ±0.1°C within the measurement. The data obtained at higher frequencies were strongly affected by the ITO relaxation [16,17], therefore, data at $f > 10$ MHz are omitted.

The dielectric relaxation phenomena for both the samples in the nematic phase were examined using the Cole-Cole relation. The Cole-Cole [18] equation is given by

$$\varepsilon^* = \varepsilon'(\infty) + \frac{\delta\varepsilon'}{1 + (j\omega\tau)^{1-\alpha}} \tag{1}$$

where $\delta\varepsilon'$ is the dielectric strength of the relaxation and $\varepsilon'(\infty)$ is the high-frequency limit of the relative dielectric permittivity, $\omega(=2\pi f)$ is the angular frequency, and τ is the relaxation time.

The low- and high-frequency deviations in dielectric data require correction for low- and high-frequency values. On separating the real and imaginary part of

Eq. (1) one may get

$$\varepsilon' = \varepsilon'(\mathrm{dc})\mathrm{f}^{-\mathrm{n}} + \varepsilon'(\infty) + \frac{\delta\varepsilon'[1 + (2\pi f\tau)^{(1-\alpha)}\sin(\alpha\pi/2)]}{1 + (2\pi f\tau)^{2(1-\alpha)} + 2(2\pi f\tau)^{(1-\alpha)}\sin(\alpha\pi/2)} \tag{1a}$$

and

$$\varepsilon'' = \frac{\sigma(dc)}{\varepsilon_0 2\pi f^k} + \frac{\delta\varepsilon'(2\pi f\tau)^{(1-\alpha)}\cos(\alpha\pi/2)}{1 + (2\pi f\tau)^{2(1-\alpha)} + 2(2\pi f\tau)^{(1-\alpha)}\sin(\alpha\pi/2)} + Af^m \tag{1b}$$

Here, $\sigma(dc)$ is the ionic conductance and ε_o is the free space permittivity; k, A, and m are the fitting parameters; α is the distribution parameter and ω is the angular frequency. The term $\varepsilon'\,(dc)/f^{-n}$ and $\sigma(dc)/\varepsilon_0 2\pi f^k$ are added in the above equation for the low-frequency effect due to the electrode polarization, capacitance, and ionic conductance. The term Af^m is added in Eq. (1b) for the high-frequency effect due to the ITO resistance and lead inductance [16,17]. By the least-squares fitting of the above equation into the experimental data we have removed the low- and high-frequency errors.

Results and Discussion

Figure 2 is the TEM Image of ZONPs used for preparing the ZONPs nematic suspension. It confirms the almost rod shape of the ZONPs, which makes it compatible for doping in rod-shaped nematic LC molecules [14].

The static dielectric permittivity ε' and dielectric loss ε'' of the pure and the ZONPs-doped LCs measured at 30°C as function of frequency for $E||n$ (electric field parallel to the director) and $E \perp n$ (electric field perpendicular to the director) orientations are shown in Figs. 3 and 4.

The values $\varepsilon_{\mathrm{II}}$ and $\varepsilon_{\perp}$ represent the relative permittivities for the applied electric field E parallel and perpendicular to the macroscopic molecular orientation $\boldsymbol{n}$,

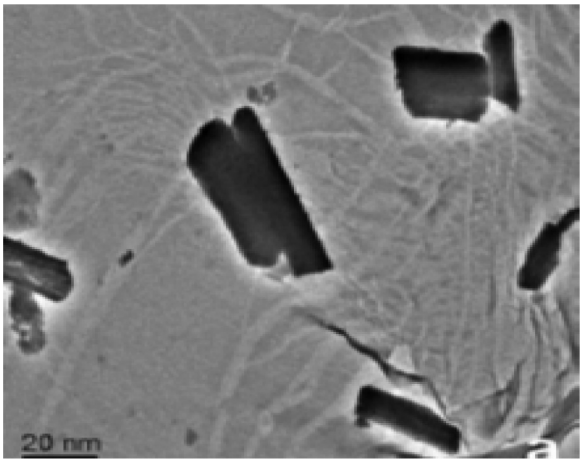

Figure 2. TEM images of ZnO nanoparticles.

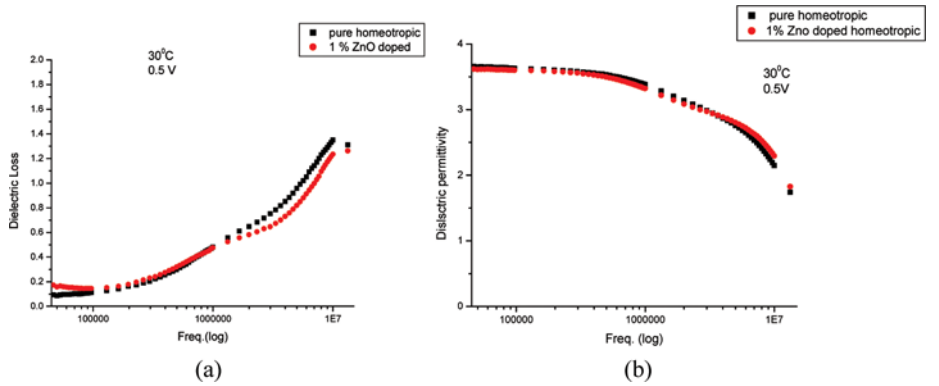

Figure 3. (a) and (b) Dielectric loss and dielectric permittivity relaxation curves for homeotropic alignment ($E||n$).

respectively. The relative permittivity is either constant or decreases with frequency. Low values of ε' at higher frequencies suggest that the molecules rotate about their molecular axis or some of the side groups rotate and give rise to this kind of relaxation [19,20]. This type of low-frequency relaxation has also been reported by other workers for nematic liquid crystals [21]. It is worth noting that the parallel component of dielectric permittivity of the pure LCs is distinctly higher than the perpendicular one for the ZONPs-doped nematic LCs.

The nature of loss curves are similar for pure and ZONPs-doped LCs. It is evident from Figs. 3 and 4 that the peaks of the curves obtained for pure and ZONPs-doped LCs have not shifted significantly in both homeotropic and planar alignments. This suggests that the relaxation frequency of ZONPs-doped LCs is similar to that of pure LCs. The reason can be attributed to the type of nanoparticles used and compatibility of nanoparticles with the LC host in perpendicular and planar alignments [12,13,20].

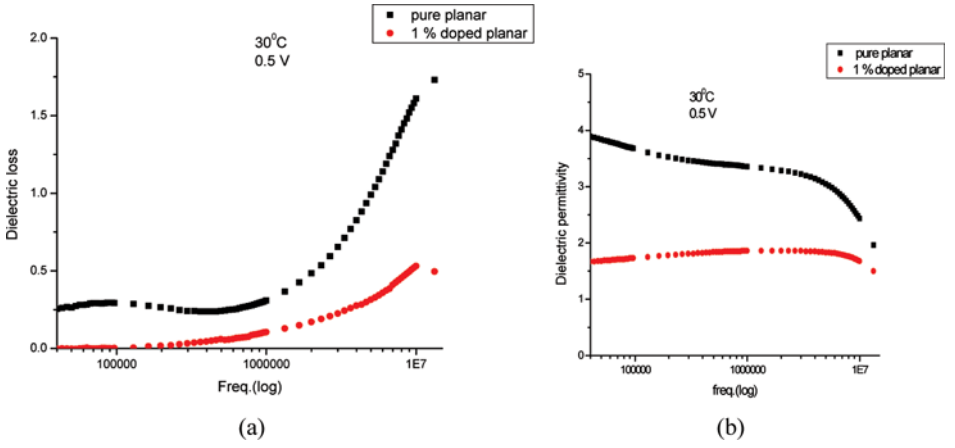

Figure 4. (a) and (b) Dielectric loss and dielectric permittivity relaxation curves for the planar alignment ($E \perp n$).

Dielectric permittivity and loss curves for homeotropic alignment are given in Fig. 3. It was found that D6AOB has two clear molecular relaxation processes in the anisotropic phase. The first process in pure D6AOB with homeotropic alignment has a characteristic frequency of 1 MHz, and the second process has a characteristic frequency of about 10 MHz. The lowest frequency mode is contributed by the longitudinal and the higher frequency mode is contributed by the transversal components of the dipole moment, respectively [22].

The frequency dependence of the dielectric permittivities for the D6AOB and ZONPs-doped D6AOB sample in the nematic phase for planar alignment is shown in Fig. 4. The relaxation processes observed in the planar alignment are qualitatively different from those in the homeotropic alignment, as can be seen by comparing Figs. 3 and 4. Even though in the homeotropic process there may exist a slow collective relaxation process due to the orientation of permanent dipoles at the nanoparticles LCs interface. In the case of D6AOB the dipole moment is much weaker than 5CB and 7CB, and the dipolar part of the molecules is situated closer to its center, with the molecules being nearly symmetric in structure. The dipole moment is at an angle around 64.9° from the long axis of the molecule. It is possible that the interaction between the dipole moment of D6AOBs and permanent polarization of ZONPs [5] causes a planar alignment of the molecules with a pretilt at the surface [12,13].

Dielectric Anisotropy

The anisotropy and its dependence on frequency $[\Delta\varepsilon(\omega) = \varepsilon_{II} - \varepsilon_{\perp}]$ are usually explained within the framework of orientation of dipoles. In our case, $\varepsilon_{\perp}$ and ε_{II} correspond to the mechanism of nematic LC dipole polarization connected with rotations of rigid bar-shaped molecules around the long and short axes respectively [23].

In the nematic phase the substances exhibit a positive dielectric anisotropy, $\Delta\varepsilon = \varepsilon_{II} - \varepsilon_{\perp} > 0$ at low frequencies as shown in Fig. 5. However, at MHz frequencies,

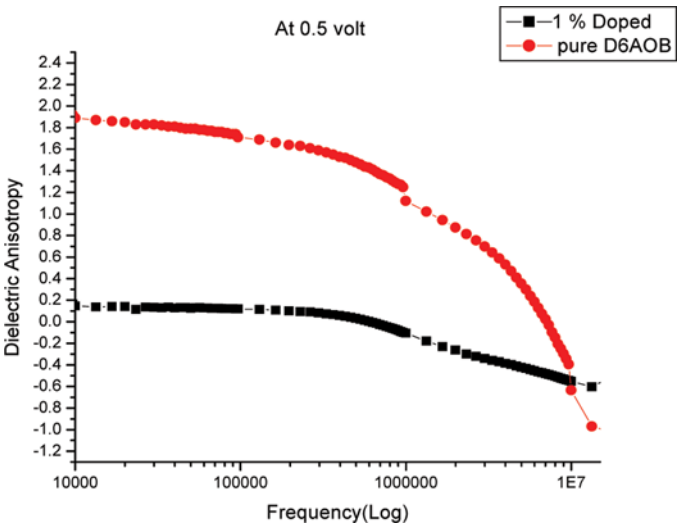

Figure 5. Frequency dependence of the dielectric anisotropy for pure and doped samples.

$\Delta\varepsilon$ decreases significantly and ultimately changes its sign for both pure D6AOB and ZONPs-doped suspension. But the sign reversal of dielectric anisotropy in a doped sample arises just before the mega-Hertz region compared to the pure sample and its value changes from $+0.2$ to -0.2 around 1 MHz. This is due to the dispersion of the parallel dielectric permittivity component and a flat behavior of the perpendicular component over a broad range of the frequency. Such behavior of the dielectric anisotropy has been also earlier reported for other LCs compounds having different chemical structures. Thus, the doped sample enables effective dual addressing of the displays due to sign reversal of dielectric anisotropy before the MHz region compared to the pure sample, which is around 10 MHz [24–26].

According to Maier and Meier [9], the dielectric anisotropy is given by

$$\Delta\varepsilon = \varepsilon_{\amalg} - \varepsilon_{\perp} = \frac{N_0 hF}{\varepsilon_0}\left\{\Delta\alpha.S - \frac{F\mu^2}{2KT}(1 - 3Cos^2\beta)S\right\} \tag{2}$$

where ε_0 is the permittivity of free space, N_0 is the number density ($= N_A\ \rho/M$; $M =$ molar mass, $\rho =$ density, $N_A =$ Avogadro number), $\Delta\alpha$ is molecular polarizability, K is the Boltzmann constant, and S is the order parameter. The local field factors h and F are dependent upon the mean dielectric permittivity $<\varepsilon>$, $<\varepsilon> = (\varepsilon_{\text{II}} + 2\varepsilon_{\perp})/3$.

The estimation of angle β between the long molecular axes and the dipole moment of the molecules for the pure and the doped sample were done using the following approach. If β changes, the dielectric anisotropy will also change according to Eq. (2).

By applying the Onsager equation [9,25]

$$\frac{(\varepsilon_s - \varepsilon_\infty)(2\varepsilon_s + \varepsilon_\infty)}{\varepsilon_s(\varepsilon_\infty + 2)^2} = \frac{N_0}{3\varepsilon_0}\frac{\mu^2}{3KT} \tag{3}$$

where ε_s and ε_∞ are the static and high-frequency permittivities, respectively, corresponding to a particular relaxation process in the Cole-Cole diagrams.

The Cole-Cole plots show the semi-circle indicating a relaxation phenomenon. The semi-circle on lower frequency side is for lateral component μ_l dipole moment and the other one is due to transverse component. With the help of Eq. (3) and the Cole-Cole plot of Fig. 6, one can obtain the expression for μ_t and μ_l (transverse and lateral component of dipole moment). The values of increment of dielectric permittivity are obtained from the Cole-Cole plot of Fig. 6. Hence, from Fig. 7 the angle $\beta = \tan^{-1}(\mu_t/\mu_l)$ can be calculated [25]. The angle β for molecules of pure D6AOB sample was found to be 64.5°, which is in good agreement with the earlier reported value [12,13]. The value of β for the molecules in the ZONPs-doped LC suspension was found to be 75°. This means that the angle β for the molecules in the doped sample increased. In other words, the resultant dipole moment of the LC molecule attained a new orientation with respect to the long molecular axis. Therefore, it can be concluded that the ZONPs significantly influenced the geometrical orientation of the D6AOB molecules in the suspension. In light of Eq. (2), we can say that on increasing the value of β, dielectric anisotropy of the doped sample is decreased with respect to the pure sample.

Further, it is seen that ε_{II} increases gradually with decreasing temperature for all samples, which is due to the increasing nematic order [12]. Hence, dielectric anisotropy $\Delta\varepsilon$ obtained from the values of dielectric permittivities below the isotropic

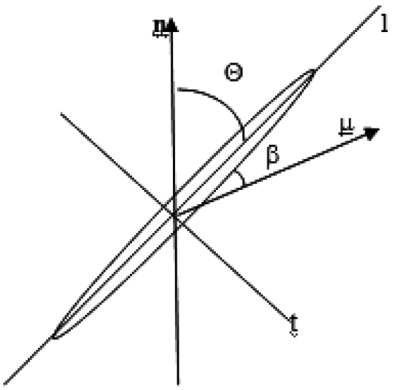

Figure 6. Schematic diagram representing angle β between the long molecular axis (**n**) and dipole moment (**μ**) of the nematic liquid-crystal molecule. Here **n** denotes the direction of macroscopic nematic orientation. The subscripts *l* and *t* denote the molecular long and short axes, respectively [27].

(I) to nematic (N) phase transition was found to increase with decreasing temperature as shown in Fig. 8.

This is due to the contribution of the electronic polarizability to ε', which is greater in the direction along the molecular long axis than perpendicular to it. For D6AOB there is an additional permanent dipole moment, which contributes slightly more in the perpendicular direction than in the parallel alignment. The decrease in dielectric anisotropy is caused by a decrease in the value of ε_{II} with increasing temperature, whereas the $\varepsilon_{\perp}$varies in a irregular manner. The decrease of ε_{II} in the ZONPs-doped sample results from the smaller distance between the molecules, leading to an increased antiparallel correlation between the component of the dipole moment along the molecular axis. Consequently, the effective dipole moment is reduced, causing a decrease in ε_{II}. The absolute value of ε_{II} and $\varepsilon_{\perp}$of D6AOBs with weak dipole moment is much smaller than for LCs with a strong dipole moment such as 5CB, which has values 18.5 and 7.0 at room temperature for parallel and perpendicular components, respectively [12,13].

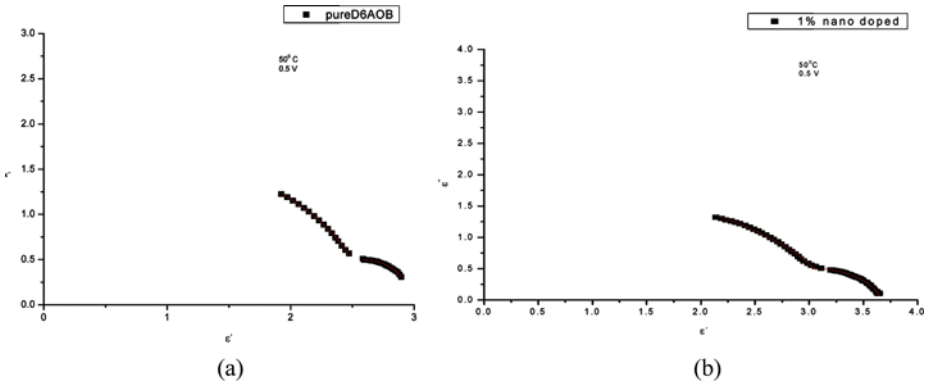

Figure 7. (a) and (b) Cole-Cole plots for homeotropic alignment of pure and ZONPs-doped samples near the isotropic phase.

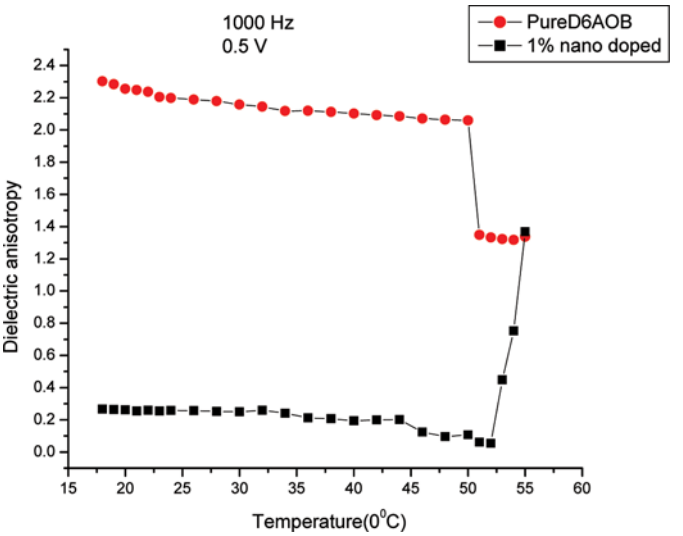

Figure 8. Variation of dielectric anisotropy with temperature for both samples [12,13].

In the doped sample the effect of nanoparticles was enough to affect the director of the phase, which prevented the alignment of the director in the field direction; hence, because in this case, the value of ε_{II} obtained in close to the average value $(\varepsilon_{II} + 2\varepsilon_{\perp})/3$ because molecules would have deviated in their orientation around ZONPs. We have also observed the dielectric anisotropy with variation of different bias voltages, as we are well aware that with the field-induced reorientation of the pure LC director in a planar-aligned cell the molecules orient themselves to the plane of the cell. An electric field applied perpendicular to the cell interacts with the dielectric anisotropy of the LC system and forces the molecules with the positive dielectric anisotropy to align in the direction of the field, thereby achieving homeotropic alignment.

In an ideal homeotropic orientation, the molecules align perpendicular to the cell plane. A sufficient field is needed to obtain a fully vertically aligned status. Above the threshold as we increase the voltage, the dipoles (D6AOBs makes an angle of 64.9° with that of the long molecular axis and in ZONPs the spontaneous polarization is along the C-axis of the particles) try to align in the field direction [5]. At a particular voltage the dipole moment of the guest and the host become aligned in the field direction [28,29]. But the long molecular axis of the guest and the host at this stage make an angle to each other, which is the result of interaction of dipole moments of the guest and the host particles, that is, the molecules of D6AOBs and ZONPs are not completely aligned in parallel. At this stage the conclusion should be that on increasing the voltage, the anisotropy of the suspension might gradually became constant above the threshold voltage as reported earlier [30]. The effect of ZONPs on the dielectric anisotropy of the suspension with variation of voltage can be seen on comparing the plot of $\Delta\varepsilon$ versus V for pure D6AOBs and doped D6AOB as shown in Fig. 9. We see that the dielectric anisotropy of the pure D6AOBs sample has not considerably changed on varying the voltage; that is, it acquires a saturation value above the threshold voltage. But the anisotropy of the doped sample decreases gradually

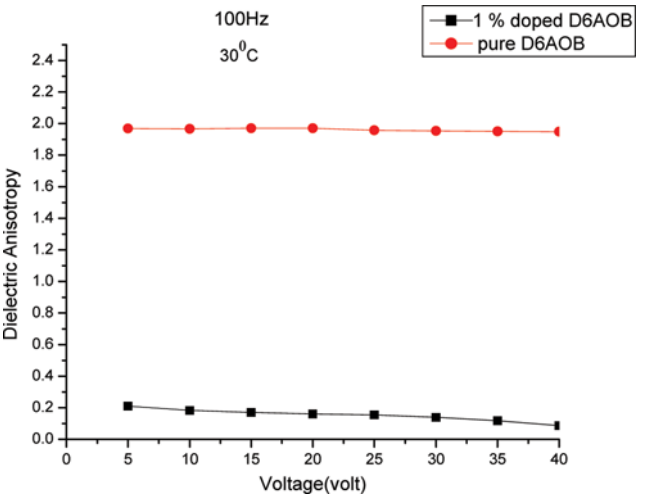

Figure 9. Variation of dielectric anisotropy with voltage.

with increasing voltage. This nature of anisotropy can be explained on the basis of a new approach as follows.

New Approach for Dielectric Anisotropy

Recently a new phenomenon of superelectrotative elongation of carbon nanotube (CNT) aggregate was observed in a superfluorinated nematic LC. The reported elongation in terms of actuation strain reached up to 400% by an in-plane actuation electric field of 5.67 $V\mu m^{-1}$ at 60 Hz, and the original shape was restored by removal of the field. The resultant piezoelectric constant, defined as the ratio of the actuation strain to the actuation field, was calculated to be several hundred times larger than a typical piezoelectric polymer. As a consequence, the CNT aggregate resembled an elastomer substance with a high expansion coefficient [31].

Because ZONPs show good piezoelectricity when they are subjected to an external electric field, rod-shaped ZONPs may have similar behavior as CNTs in the pure D6AOB sample. Hence, in the external field condition the ZONPs may change their shape as shown in Fig. 10. The slight shape change of the particles (in our case ZONPs) during an applied electric field above the threshold cause a change in the stability of the surrounding liquid-crystalline phase [32].

Therefore, the liquid-crystalline order is somewhat destroyed. This effect obviously causes the decrease in the anisotropy on increasing voltage above the threshold. Hence, the hypothesis of isotropization [33] is found in our experimental

Figure 10. ZONPs (nanorods) in the nematic LC above the threshold field.

results of anisotropy. Isotropization is a consequence of the disorder that is introduced by the guest particles in the liquid-crystalline phase. The ZONPs network divides the LC molecules over domains, which in course disrupts the long-range liquid-crystalline order. This means that the structure, and consequently the molecular dynamics, will be driven toward a more isotropic order. One of the effects of the liquid-crystalline order is a retardation of the rotation of short axis compared to the isotropic phase. If the order is disrupted, this rotation should become faster, evolving in the direction of the isotropic value with increasing disorder [33,34]. This piezoelectric effect of nanoparticles on LC molecules provides a new way of research.

Conclusion

The results of dielectric studies performed for pure D6AOB nematic LC and ZONPs doped nematic LC allow us to suggest the following:

1. The two relaxation processes have been explained on the basis of the rotation of the molecule along the short and long molecular axes in pure and doped samples.
2. The phenomenon of sign reversal of dielectric anisotropy in a doped sample occurs before the MHz region of frequency compared to the pure sample. This fact is very useful for effective design of dual-addressing displays.
3. The angle β increases for the doped sample and hence the dielectric anisotropy for the doped sample decreases, which provides a way to obtain the desired anisotropy of the system by doping definite concentrations of nanoparticles. With the help of the Onsager theory, near the phase transition temperature this angle could be estimated from the Cole-Cole plots of the pure and doped samples.
4. The behavior of anisotropy with temperature, that is, with decreasing temperature the anisotropy increases, is well explained on the basis of increasing nematic order for both pure and doped samples.
5. The anisotropy of the doped sample decreases with increasing voltage, whereas for the pure sample it remains constant. This deduction in dielectric anisotropy for the doped sample with increasing voltage could be explained on the basis of piezoelectric strain of the nanoparticles.

Acknowledgments

The author is sincerely thankful to CSIR (New Delhi, India) for providing the financial support in the form of SRF. The authors are also thankful to Sponsored Research, Indian Space Research Organization for providing grant in the form of project.

References

[1] Heng, M., Rui-Zhi, S., Zhen-Xin, L., & Yu-Fang, L. (2008). *Chin. Phys., B*, *17*, 255.
[2] Gangal, S. V. (1989). *Encyclopaedia of Polymer Science*, Wiley-Inter Science: New York.
[3] Haraguchi, F., Inoue, K., Toshima, N., Kobayashi, S., & Takatoh, K. (2007). *Jpn. J. Appl. Phys.*, *46*, L796.
[4] Brochard, F., & de Gennes, P. G. (1970). *J. Phys.*, *31*, 691.
[5] Zhong, L. W. (2004). *Mater. Today*, *6*, 26.

[6] Landi, B. J., Roffaelle, R. P., Heben, M. J., Alleman, J. L., Derveen, W. V., & Gennett, T. (2002). *Nano Lett.*, *2*, 1329.
[7] De Gennes, P. G., & Prost, J. (1997). *The Physics of Liquid Crystals*, Oxford University Press: New York.
[8] Wu, S. T., & Yang, D. K. (2006). *Fundamentals of Liquid Crystal Devices*, John Wiley: New York.
[9] Blinov, L. M., & Chigrinov, V. G. (1994). *Electro Optic Effects in Liquid Crystal Materials*, Springer-Verlag: New York.
[10] George, A. K., Hinani, M. A., Potukuchi, D. M., Alharthi, S. H., & Carboni, C. (2003). *Phase Transitions*, *76*, 1037.
[11] Anisimov, M. A. (1987). *Mol. Cryst. Liq. Cryst.*, *146*, 435.
[12] Sinha, G., Oka, A., Glorieux, C., & Thoen, J. (2004). *Liq. Cryst.*, *31*, 1123.
[13] Oka, A., Sinha, G., Glorieux, C., & Thoen, J. (2004). *Liq. Cryst.*, *31*, 31.
[14] Sharma, P. K., Kumar, M., & Pandey, A. C. (2009). *Acta Materialia*, *1*, 1117.
[15] Srivastava, A. K., Misra, A. K., Chand, P. B., Manohar, R., & Shukla, J. P. (2007). *Phys. Lett. A.*, *371*, 490.
[16] Misra, A. K., Srivastava, A. K., Shukla, J. P., & Manohar, R. (2008). *Phys. Scr.*, *78*, 065602-1.
[17] Manohar, R., Misra, A. K., Srivastava, A. K., Chand, P. B., & Shukla, J. P. (2007). *Soft Mater.*, *5*(4), 207.
[18] Cole, K. S., & Cole, R. H. (1941). *J. Chem. Phys.*, *9*, 341.
[19] Pasechnik, S. V., Chigrinov, V. G., Shmeliova, D. V., Tsvetkov, V. A., Kremenetsky, V. N., Zhijian, L., & Dubtsov, A. V. (2006). *Liq. Cryst.*, *33*, 175.
[20] Pal, D., Mishra, P., Misra, A. K., Manohar, R., & Shukla, J. P. (2007). *Res. J. Phys.*, *1*(1), 10.
[21] Biradar, A. M., Kilian, D., & Hasse. W. (2000). *Liq. Cryst.*, *27*, 225.
[22] Merkel, K., Kocot, A., Vij, J. K., Mehl, G. H., & Meyer, T. (2006). *Phys. Rev. E.*, *73*, 051702-1.
[23] Belyaev, B. A., Drokin, N. A., Shabanov, V. F., & Shepov, V. N. (2000). *Phys. Solid State*, *42*, 577.
[24] Czub, J., Dabrowski, R., & Urban, S. (2007). *Phase Transitions*, *80*, 631.
[25] Czub, J., Urban, S., Geppi, M., Marini, A., & Dabrowski, R. (2008). *Liq. Cryst.*, *35*, 527.
[26] Jankowiak, A., Januszko, A., Ringstrand, B., & Kaszynski, P. (2008). *Liq. Cryst.*, *35*, 65.
[27] Jadzyn, J., Czerkas, S., Czechowski, G., Burczyk, A., & Dabrowsky, R. (1999). *Liq. Cryst.*, *26*, 437.
[28] De Jeu, W. H., Lathouwers, T. W., & Bordewijk, P. (1974). *Phys. Rev. Lett.*, *32*, 40.
[29] De Jeu, W. H. (1980). In: *Physical Properties of Liquid Crystalline Materials*, Gray, J. W. (Ed.), Gordon and Breach, Ch. 5.
[30] Xu, H., Trushkevych, O., Collings, N., & Crossland, W. A. (2009). *Mol. Cryst. Liq. Cryst.*, *502*, 235.
[31] Rahman, M., & Lee, W. J. (2009). *Phys. J: Appl. Phys.*, *42*, 063001-1.
[32] Allinson, H., & Gluson, H. F. (1995). *Liq. Cryst.*, *19*, 421.
[33] Leys, J., Glorieux, C., & Thoen, J. (2008). *J. Phys. Condens. Matter.*, *20*, 244111-1.
[34] Sinha, G., Leys, J., Glorieux, C., & Thoen, J. (2005). *Phys. Rev. E.*, *72*, 051710-1.